

Novel high-pressure phase with pseudo-benzene “N₆” molecule of LiN₃

MEIGUANG ZHANG^{1(a)}, HAIYAN YAN², QUN WEI³, HUI WANG^{4,5} and ZHIJIAN WU^{5(b)}

¹ Department of Physics and information Technology, Baoji University of Arts and Sciences
Baoji 721016, China

² College of Chemistry and Chemical Engineering, Baoji University of Arts and Sciences
Baoji 721013, China

³ School of Science, Xidian University - Xi'an 710071, China

⁴ National Laboratory of Superhard Materials, Jilin University - Changchun 130012, China

⁵ Key Laboratory of Rare Earth Chemistry and Physics, Changchun Institute of Applied Chemistry,
Chinese Academy of Sciences - Changchun 130022, China

received 2 December 2012; accepted in final form 14 January 2013

published online 6 February 2013

PACS 61.50.Ks – Crystallographic aspects of phase transformations; pressure effects

PACS 71.15.Mb – Density functional theory, local density approximation, gradient and other corrections

PACS 71.20.-b – Electron density of states and band structure of crystalline solids

Abstract – The pressure-induced formation of a hexagonal phase ($P6/m$, $Z=2$) of LiN₃ is predicted by particle swarm optimization (PSO) structural search at zero temperature and pressure of > 34.7 GPa. Compared to the ground-state insulator $C2/m$ phase, the $P6/m$ -LiN₃ is found to possess a metallic feature dominated by the $2p_z$ bands. Electron topological analysis revealed an intriguing phase change of nitrogen, from azide to novel pseudo-benzene “N₆” molecules at the formation of the $P6/m$ phase. The occurrence of this hexagonal phase follows the polymerization of the typical linear N₃[−] anion molecular chains in the low-pressure molecular phases of LiN₃ and is originated from the volume reduction favorable for a denser structure packing under compression.

Copyright © EPLA, 2013

Introduction. – Alkali metal azides, typical molecular crystals constructed by spherical cations and linear-rod-shaped anions, have attracted much attention due to their unique physical and chemical properties in technological applications and fundamental science. Apart from their industrial usefulness as pure nitrogen sources, initial explosives, and photographic materials [1]. Alkali metal azides are also model systems [2] for studying the main regularities of fast chemical reactions in solids with complex chemical bonding as their spatial symmetry and internal molecular structure (a linear molecular N₃[−] anion) make them logical candidates for such studies following alkali halides and cyanides. Extensive experimental and theoretical studies have been undertaken on the structural, electronic, and optical properties of alkali metal azides.

Recently, high-pressure studies on alkali metal azides have been of special interest because of their use as a

precursor in the formation of polymeric nitrogen —the ultimate example of a high energy density material (HEDM). This is pioneered by studies of nitrogen [3], of which, the polymeric cubic gauche (*cg*) atomic phase was successfully synthesized under high pressure and high temperature. Experimentally, the high-pressure behaviors of LiN₃ [4], NaN₃ [5], KN₃ [6,7], and CsN₃ [8] have been intensively studied by using Raman spectroscopy and X-ray diffraction techniques. The N₃[−] anions in NaN₃ were found to transform to a non-molecular nitrogen state with an amorphous-like structure when compressed to 120–160 GPa [5]. More recently, the pressure-induced structural transition sequence of CsN₃ up to 54.4 GPa was determined by Hou *et al.* [8]. Simultaneously, Cheng *et al.* [6,7] predicted a structural phase transition of KN₃ at a pressure of 15.5 GPa by *in situ* synchrotron powder X-ray diffraction. However, Medvedev *et al.* [4] reported that LiN₃ is stable up to 60 GPa at ambient temperature, which is in contrast to that of NaN₃, KN₃, and CsN₃. Subsequently, density functional theory calculations [9]

(a) E-mail: zhmgbj@126.com

(b) E-mail: zjwu@ciac.jl.cn

about the structural, electronic, optical, and vibrational properties of LiN_3 have been investigated up to 60 GPa, and the results do not suggest structural transformations during this pressure range. Therefore, the peculiarity and the absence of a characterized high-pressure phase of LiN_3 prompted our endeavor to investigate its structural behavior at higher pressure. Furthermore, the exploration of the phase transition behavior of LiN_3 would provide further insight into the pressure effect on the rearrangement of the N_3^- anions and phase transitions that might result in the formation of polymeric nitrogen.

Here, we presented extensive structure searches to uncover the high-pressure structures of LiN_3 based on a global minimization of free-energy surfaces merging *ab initio* total energy calculations via the PSO technique [10,11], as implemented in the Crystal structure AnaLYsis by Particle Swarm Optimization (CALYPSO) code [12]. This methodology has been successfully applied to many high-pressure structures on elements, binary, and ternary compounds [13–18], among which the blind prediction of high-pressure orthorhombic structure of FeTi_3O_7 [16], two low-pressure monoclinic structures of Bi_2Te_3 [17], and insulating Aba2-40 (or oC40) structure of dense Li [18,19] have been confirmed by independent experiments. In the present work, we predicted a novel simple hexagonal structure (space group $P6/m$) with exotic pseudo-benzene “ N_6 ” ring, as the energetically most stable phase in pressure region of 34.7–200 GPa. The N_3^- anions in this hexagonal phase kept their molecular character in this pressure range. Therefore, the complete polymerization of nitrogen in LiN_3 may occur far beyond 200 GPa.

Computational methods. – The variable-cell high-pressure structure predictions were performed at pressures in the range of 0, 25, 50, 100, and 200 GPa with systems containing one to four formula units (f.u.) in the simulation cell as implemented in the CALYPSO code [12]. The underlying *ab initio* structure relaxations were performed using density functional theory within the Perdew-Burke-Ernzerhof parameterization of the Generalized Gradient Approximation (GGA) [20] as implemented in the VASP code [21]. The electron and core interactions were included by using the frozen-core all-electron projector augmented wave (PAW) method [22], with N: $2s^22p^3$, and Li: $1s^22s^1$, treated as the valence electrons. The energy cutoff 520 eV and appropriate Monkhorst-Pack k meshes [23] were chosen to ensure that enthalpy calculations are well converged to better than 1 meV/atom. The charge density topology was analyzed based on Bader’s quantum theory of Atoms-in-Molecules (AIM) [24]. The phonon calculations were carried out by using a supercell approach as implemented in the PHONOPY code [25].

Results and discussion. – At ambient pressure, LiN_3 adopts the monoclinic structure (space group $C2/m$, $Z=2$, fig. 1(a)), which is isostructural to the low-temperature phase of NaN_3 [26]. For $C2/m$ - LiN_3 , the N_3^- anion axes are parallel to each other and tilted by a

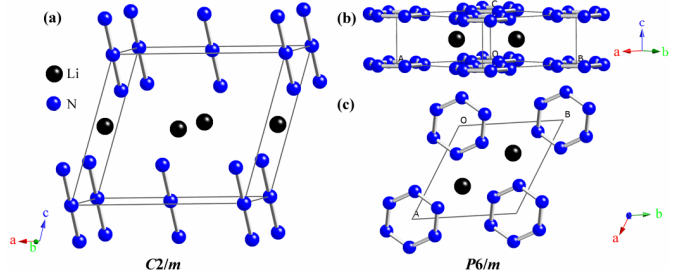


Fig. 1: (Color online) Crystal structures of $C2/m$ - LiN_3 (a), $P6/m$ - LiN_3 (b), and c -axis projection view of $P6/m$ - LiN_3 (c); the black and blue spheres represent Li and N atoms, respectively.

certain angle within the layers in which they are stacked. Therefore, one expects more luxuriant rearrangements of N_3^- anions and the possible formation of polymeric nitrogen under higher pressure. At 0 and 25 GPa, our simulations with the only input of chemical composition of Li : N = 1 : 3 predicted the most stable structure to be the monoclinic $C2/m$ structure. This sheds a strong light on the validity of the CALYPSO methodology used in the structural searches. At higher pressure, the most stable hexagonal $P6/m$ phase (fig. 1(b) and fig. 1(c)) with two f.u. in a unit cell was found at 50, 100 and 200 GPa, respectively. This structure is characterized by an intriguing N-Li-N sandwiches stacking order. The formation of hexagonal $P6/m$ phase with N layers resulted from the strong distortion of the linear N_3^- anions of the $C2/m$ phase and the concomitant displacement of Li atoms. The parallel arrangement of N_3^- anions in the $C2/m$ phase collapsed into planar nets under compression and formed exotic pseudo-benzene “ N_6 ” rings which are more favorable in the $P6/m$ phase. At 50 GPa, this $P6/m$ phase has the optimized lattice parameters $a = b = 4.918 \text{ \AA}$ and $c = 2.376 \text{ \AA}$ with atomic positions: N atoms at $6j$ (0.191, 0.305, 0) and Li atoms at $2d$ ($1/3$, $2/3$, $1/2$). In more detail, the pseudo-benzene “ N_6 ” molecule with the N-N distance of 1.313 \AA is parallel to the ab plane and located between the adjacent graphite-like Li layers, in which each Li atom has six nearest N neighbors with a Li-N bond length of 1.954 \AA . At zero temperature a stable crystalline structure requires all phonon frequencies to be positive. We have calculated the phonon dispersion curves of $P6/m$ - LiN_3 at 150 GPa as shown in fig. 2(a). No imaginary phonon frequencies are found in the whole Brillouin zone, indicating the dynamical stability of this new hexagonal high-pressure phase. Furthermore, the primitive cell of $P6/m$ structure contains 8 atoms, giving 24 phonon branches. The calculated zone-center (Γ) phonon eigenvectors were used to deduce the symmetry labels of phonon modes. The group theory analysis shows that the 24 vibrational modes of $P6/m$ at the zone center have the irreducible representations $\Gamma_{P6/m} = 2(A_g^R + A_u^I + B_g + B_u) + 3(2E_{2g}^R + 1E_{1u}^I + 1E_{2g}^R + 2E_{1u}^I) + (2E_{2u} + 1E_{1g}^R + 1E_{2u} + 2E_{1g}^R)$.

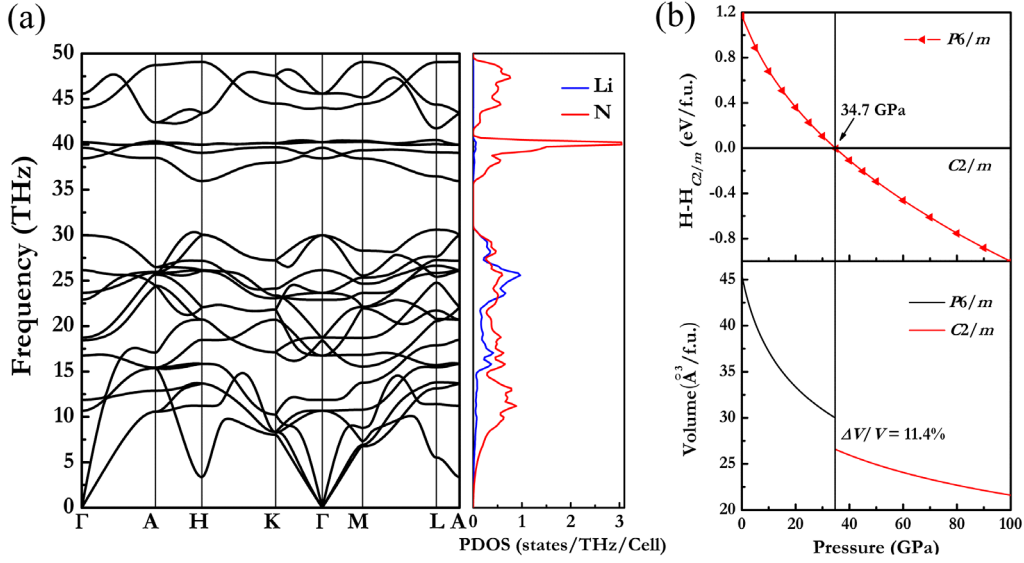


Fig. 2: (Color online) Phonon dispersion curves of the $P6/m$ -LiN₃ at 150 GPa (a); enthalpy of the $P6/m$ -LiN₃ relative to the $C2/m$ -LiN₃ as a function of pressure and calculated volumes as a function of pressure (b).

The Raman active modes are labeled by superscript R and infrared active modes by I. The Raman and infrared frequencies of the structure (zone-center phonons in fig. 2(a)) could be useful for the future experiments to identify the $P6/m$ structure of LiN₃.

Our computational method is based on constant-pressure static quantum-mechanical calculations at $T = 0$ K, so the Gibbs free energy is reduced to enthalpy. To determine the phase transition pressure, we have plotted out the enthalpy curves of the predicted $P6/m$ -LiN₃ relative to the ambient pressure $C2/m$ -LiN₃ in fig. 2(b). The recent reported high-pressure $I4/mcm$ structure of CsN₃ [8] was also considered for comparison. It is confirmed from fig. 2(b) that the $P6/m$ -LiN₃ becomes more stable than the $C2/m$ -LiN₃ phase above 34.7 GPa. Compared to the $P6/m$ -LiN₃, the $I4/mcm$ structure of CsN₃ possesses larger enthalpy values in the studied pressure ranges and thus it is not shown here. One question is naturally raised associated with the too low phase transition pressure (34.7 GPa) in LiN₃, which contradicts the experimentally reported stability of the $C2/m$ phase up to 60 GPa [4]. We here, however, provide two possible arguments. Firstly, we did not include the temperature effect in the calculation, but experiences tell us that room temperature is not too high to significantly revise the transition pressure. Secondly, we suspect that there exists a certain energy barrier for this phase transition, originated from the enhanced repulsive interactions between the N₃⁻ anions under the increasing the compression and extra pressure is needed to overcome this barrier. For the second respect, it has been elaborated in high-pressure experiments of LiN₃ and CsN₃ [4,8]. As reported in ref. [4] for $C2/m$ -LiN₃, the angular amplitude of the torsional motion of N₃⁻

anions displacement from equilibrium becomes especially insignificant under increasing compression, indicating the strong hindering of structural rearrangement by increasing the repulsive interaction of the negatively charged end atoms of adjacent N₃⁻ anions. This resembles the high-pressure synthesis of transition metal nitrides from the elemental constituents, where much higher pressures are necessary to promote the reaction [27,28]. We also note that application of high temperature could be helpful in lowering the energy barrier for the realization of this phase transition. Another interesting result presented in the paper is that this $P6/m$ phase persists up to at least 200 GPa according to our structural predictions. This wide stable pressure range may be attributed to the smaller ionic radius of the Li atom, and chemical precompression exerted by heavier atoms (Na, K, Rb, etc.) in azides is expected to imply that lower pressures might be required to attain the structural phase transitions and the polymerization of N₃⁻ anions in these compounds. Furthermore, the calculated P - V curves (fig. 2(b)) of this high-pressure structure suggested that the phase transitions of $C2/m \rightarrow P6/m$ is of first order with volume drop of 11.4%, which can be easy to detect in further experiments.

Atomic displacements are always accompanied by a striking change of properties, especially electronic properties. Therefore, the total and site projected density of states (DOS), band structure, and electron density distribution of $P6/m$ -LiN₃ were calculated at 50 GPa, respectively. For the ambient pressure $C2/m$ phase, the calculated results suggest that it is an insulator characterized by a large energy gap of 3.7 eV (fig. 3(a)), this value is in agreement with the previous theoretical results: 3.7 eV [29], 3.46 eV [30], and 3.32 eV [9]. As can be seen

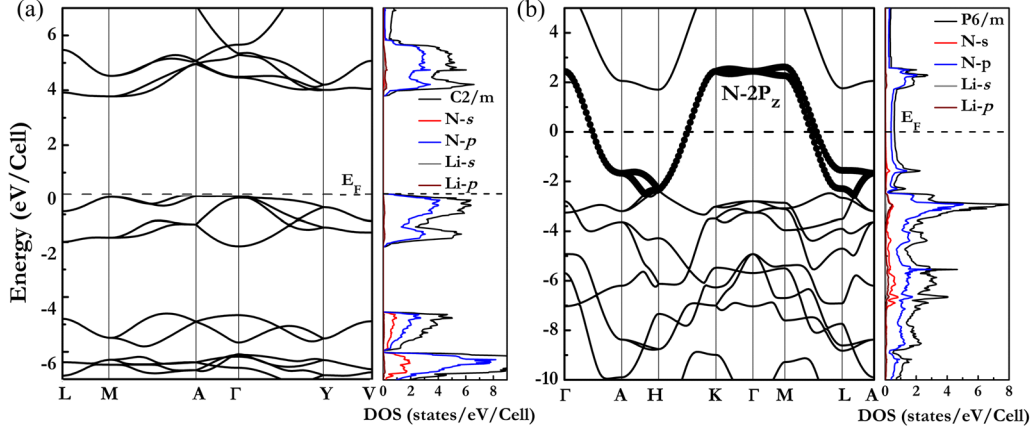


Fig. 3: (Color online) Band structure, total, and site projected density of states (DOS) of the $C2/m$ - LiN_3 at 0 GPa (a) and $P6/m$ - LiN_3 at 50 GPa (b).

from the band structure and partial DOS of $P6/m$ - LiN_3 in fig. 3(b), the $2p_z$ bands of the $P6/m$ phase cross the Fermi level along $\Gamma \rightarrow A$, $H \rightarrow K$, and $M \rightarrow L$ directions in the Brillouin zone, indicating a metallic character. The low metallization pressure of LiN_3 is in contrast to the ultra-high value for pure nitrogen [31]. The metallization in LiN_3 is in many ways similar to the metallization of hydrogen in group-IV hydrides at high pressure [32,33]. Besides, an “ionized” Li is supported by the empty Li- s state in fig. 3(b). Through Bader charge analysis, we found that the charge transfer value of $\text{Li} \rightarrow \text{N}$ is $0.85 e$ in each f.u., signifying the Li-N ionic bonding nature. Figure 4(a) further presents the calculated charge densities of the $2p_z$ bands in the Brillouin zone along the $\Gamma \rightarrow A$, $H \rightarrow K$, and $M \rightarrow L$ directions, which all correspond to the c crystallographic axis direction in real space (see fig. 4(b)). It can be seen that there exist well-defined zigzag ionic chains along the c -axis interconnected by shared Li and N atoms, which could be further confirmed by the charge density of LiN_3 in the (110) plane (in fig. 4(c)). Therefore, the c -axis can be viewed as the direction of motion of conductive carriers in this metallic $P6/m$ - LiN_3 .

In order to quantitatively describe the chemical bonding behavior of this novel hexagonal phase, electron topological analysis of $P6/m$ - LiN_3 was performed through Atoms-in-Molecules (AIM) theory [24]. The (3, -1) bond critical points (BCPs) which locate at the adjacent nitrogen atoms at pseudo-benzene “ N_6 ” ring possess negative $\nabla^2 \rho(\vec{r}_{CP})$ (Laplacian value) and large $\rho(\vec{r}_{CP})$ (local electronic density of $2.774 e\text{\AA}^{-3}$) to indicate the strong double $\text{N}=\text{N}$ covalent bonding nature. However, $\rho(\vec{r}_{CP})$ of inter-“ N_6 ” BCPs are much smaller (*i.e.*, 0.156 and $0.130 e\text{\AA}^{-3}$) and the corresponding $\nabla^2 \rho(\vec{r}_{CP})$ are all positive, suggesting a closed-shell interaction among these “ N_6 ” rings. In addition, all $\nabla^2 \rho(\vec{r}_{CP})$ at BCPs of unequivalent N and Li in $P6/m$ - LiN_3 are positive, indicating a closed-shell interaction character which is in agreement with an “ionized” Li picture presented in the partial DOS. Therefore, the N_3^- anions in $P6/m$ - LiN_3 keep their molecular character

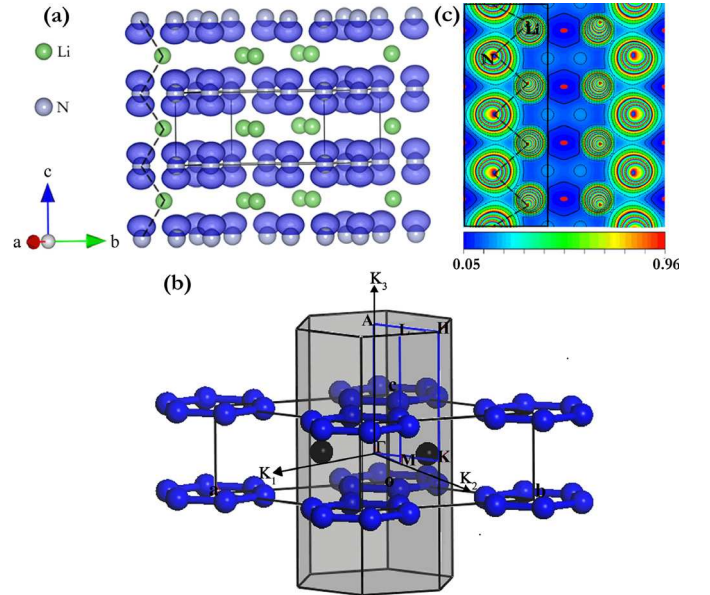


Fig. 4: (Color online) Calculated charge densities of the $2p_z$ bands along the $\Gamma \rightarrow A$, $H \rightarrow K$, and $M \rightarrow L$ directions (a), the reciprocal space of the $P6/m$ - LiN_3 (b), and charge densities of the $P6/m$ - LiN_3 in the (110) plane (c).

in the pressure range of 34.7–200 GPa. Accordingly, the complete polymerization of a nitrogen atom in LiN_3 may occur far beyond 200 GPa compared to pure nitrogen [5].

Conclusions. – In summary, we have performed a systematic exploration of the high-pressure crystal structures of LiN_3 up to 200 GPa by *ab initio* calculations via the particle swarm optimization technique as implemented in the CALYPSO code. A hexagonal $P6/m$ phase is found to be most stable at low temperature in the pressure range of 34.7–200 GPa. The results suggest that $C2/m \rightarrow P6/m$ phase transition is of first order with volume drop of 11.4%. Compared to the ambient pressure insulator $C2/m$, the $P6/m$ - LiN_3 is found to have a metallic feature dominated the $2p_z$ bands. The electronic topology properties

calculations reveal that the N₃⁻ anions in *P6/m*-LiN₃ keep their molecular character. Therefore, the complete polymerization of the N atom may occur far beyond 200 GPa.

This work was financially supported by the Natural Science Foundation of China (Nos. 11204007 and 11147007), Natural Science Basic Research plan in Shaanxi Province of China (grant No. 2012JQ1005), Baoji University of Arts and Sciences Key Research (No. ZK11060), China Postdoctoral Science Foundation (No. 2012M510893), and Open Project of State Key Laboratory of Superhard Materials (Jilin University No. 201204).

REFERENCES

- [1] EVANS B. L., YOFFE A. D. and GRAY P., *Chem. Rev.*, **59** (1959) 515.
- [2] BOWDEN F. P. and YOFFE A. D. (Editors), *Fast Reactions in Solids* (Butterworth, London) 1958.
- [3] EREMETS M. I., GAVRILIUK A. G., TROJAN I. A., DZIVENKO D. A. and BOEHLER R., *Nat. Mater.*, **3** (2004) 558.
- [4] MEDVEDEV S. A., TROJAN I. A., EREMETS M. I., PALASYUK T., KLAPOETKE T. M. and EVERS J., *J. Phys.: Condens. Matter*, **21** (2009) 195404.
- [5] EREMETS M. I., POPOV M. YU., TROJAN I. A., DENISOV V. N., BOEHLER R. and HEMLEY R. J., *J. Chem. Phys.*, **120** (2004) 10618.
- [6] JI C., ZHANG F. X., HOU D. B., ZHU H. Y., WU J. Z., CHYU M. C., LEVITAS V. I. and MA Y. Z., *J. Phys. Chem. Solids*, **72** (2011) 736.
- [7] JI C., ZHENG R., HOU D. B., ZHU H. Y., WU J. Z., CHYU M. C. and MA Y. Z., *J. Appl. Phys.*, **111** (2012) 112613.
- [8] HOU D. B., ZHANG F. X., JI C., HANNON T., ZHU H. Y., WU J. Z. and MA Y. Z., *Phys. Rev. B*, **84** (2011) 064127.
- [9] BABU K. R., LINGAM CH. B., TEWARI S. P. and VAITHEESWARAN G., *J. Phys. Chem. A*, **115** (2011) 4521.
- [10] WANG Y. C., LV J., ZHU L. and MA Y. M., *Phys. Rev. B*, **82** (2010) 094116.
- [11] WANG Y. C., LV J., ZHU L. and MA Y. M., *Comput. Phys. Commun.*, **183** (2012) 2063.
- [12] MA Y. M., WANG Y. C., LV J. and ZHU L., <http://www.calypso.cn/>.
- [13] WANG H., TSE J. S., TANAKA K., IITAKA T. and MA Y. M., *Proc. Natl. Acad. Sci. U.S.A.*, **109** (2012) 6463.
- [14] ZHU L., WANG Z. W., WANG Y. C., ZOU G. T., MAO H. K. and MA Y. M., *Proc. Natl. Acad. Sci. U.S.A.*, **109** (2012) 751.
- [15] WANG Y. C., LIU H. Y., LV J., ZHU L., WANG H. and MA Y. M., *Nat. Commun.*, **2** (2011) 563.
- [16] NISHIO-HAMANE D., ZHANG M. G., YAGI T. and MA Y. M., *Am. Mineral.*, **97** (2012) 568.
- [17] ZHU L., WANG H., WANG Y. C., LV J., MA Y. M., CUI Q. L., MA Y. M. and ZOU G. T., *Phys. Rev. Lett.*, **106** (2011) 14550.
- [18] LV J., WANG Y. C., ZHU L. and MA Y. M., *Phys. Rev. Lett.*, **106** (2011) 015503.
- [19] GUILLAUME C. L., GREGORYANZ E., DEGTYAREVA O., MCMAHON M. I., HANFLAND M., EVANS S., GUTHRIE M., SINOGEIKIN S. V. and MAO H. K., *Nat. Phys.*, **7** (2011) 211.
- [20] PERDEW J. P., BURKE K. and ERNZERHOF M., *Phys. Rev. Lett.*, **77** (1996) 3865.
- [21] KRESSE G. and FURTHMÜLLER J., *Phys. Rev. B*, **54** (1996) 11169.
- [22] KRESSE G. and JOUBERT D., *Phys. Rev. B*, **59** (1999) 1758.
- [23] MONKHORST H. J. and PACK J. D., *Phys. Rev. B*, **13** (1976) 5188.
- [24] BADER R. F. W., *Atoms in Molecules: A Quantum Theory* (Oxford University Press, New York) 1990.
- [25] TOGO A. and PHONOPY, <http://sourceforge.net/projects/phonopy/>.
- [26] IQBAL Z. and CHRISTOE C. W., *Solid State Commun.*, **17** (1975) 71.
- [27] CROWHURST J. C., GONCHAROV A. F., SADIGH B., EVANS C. L., MORRALL P. G., FERREIRA J. L. and NELSON A. J., *Science*, **311** (2006) 1275.
- [28] ÅBERG D., SADIGH B., CROWHURST J. and GONCHAROV A. F., *Phys. Rev. Lett.*, **100** (2008) 95501.
- [29] PERGER W. F., *Int. J. Quantum Chem.*, **110** (2010) 1916.
- [30] GORDIENKO A. B. and POPLAVNOI A. S., *Phys. Status Solidi B*, **202** (1997) 941.
- [31] WANG X. L., WANG Y. C., MIAO M. S., ZHONG X., LV J., CUI T., LI J. F., CHEN L., PICKARD C. J. and MA Y. M., *Phys. Rev. Lett.*, **109** (2012) 175502.
- [32] ASHCROFT N. W., *Phys. Rev. Lett.*, **92** (2004) 187002.
- [33] EREMETS M. I., TROJAN I. A., MEDVEDEV S. A., TSE J. S. and YAO Y., *Science*, **319** (2008) 1506.